Heliyon 10 (2024) e23681

Contents lists available at ScienceDirect

Heliyon

journal homepage: www.cell.com/heliyon

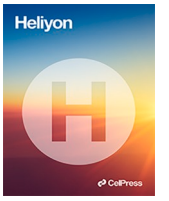

RNA-seq unravels distinct expression profiles of keloids and Dupuytren's disease

Marcus Stocks [a,1], Annika S. Walter [a,1], Elif Akova [a], Gerd Gauglitz [b], Attila Aszodi [a], Wolfgang Boecker [a], Maximilian M. Saller [a], Elias Volkmer [a,c,*]

[a] *Department of Orthopaedics and Trauma Surgery, Musculoskeletal University Center Munich (MUM), University Hospital, Ludwig-Maximillians-University (LMU), Frauenhoferstr. 12, 80336 Munich, Germany*
[b] *Department of Dermatology and Allergy, University Hospital, LMU, Thalkirchnerstr. 48, 80337 Munich, Germany*
[c] *Clinic of Hand Surgery, Helios Klinikum Muenchen West, Steinerweg 5, 81241 Munich, Germany*

A B S T R A C T

Keloid scars and Dupuytren's disease are two common, chronic, and incurable fibroproliferative disorders that, among other shared clinical features, may induce joint contractures. We employed bulk RNA sequencing to discern potential shared gene expression patterns and underlying pathological pathways between these two conditions. Our aim was to uncover potential molecular targets that could pave the way for novel therapeutic strategies. Differentially expressed genes (DEGs) were functionally annotated using Gene Ontology (GO) terms and the Kyoto Encyclopedia of Genes and Genomes (KEGG) pathways with the Database for Annotation, Visualization, and Integrated Discovery (DAVID). The protein-protein-interaction (PPI) networks were constructed by using the Search Tool for the Retrieval of Interacting Genes (STRING) and Cytoscape. The Molecular Complex Detection (MCODE) plugin was used for downstream analysis of the PPI networks. A total of 1922 DEGs were identified within Dupuytren's and keloid samples, yet no overlapping gene expression profiles were detected. Significantly enriched GO terms were related to skin development and tendon formation in keloid scars and Dupuytren's disease, respectively. The PPI network analysis revealed 10 genes and the module analysis provided six protein networks, which might play an integral part in disease development. These genes, including CDH1, ERBB2, CASP3 and RPS27A, may serve as new targets for future research to develop biomarkers and/or therapeutic agents.

1. Introduction

Keloids are abnormal proliferations of scar tissue forming at the site of cutaneous injury. They may be defined as benign fibrous skin tumors with an uncontrolled cell proliferation beyond the borders of the original wound [1,2]. Dupuytren's disease is a fibroproliferative disorder of the hands associated with an uncontrolled fibroblast growth and extracellular matrix deposition [3]. Both conditions are incurable, they both tend to chronically progress and have a certain genetic predisposition [4,5]. They both share a higher prevalence in specific ethnic groups and occur in areas of high mechanical stress [2,3]. Both diseases may induce contractures. Often times, surgery is necessary to improve function of the affected limb despite not being a definite cure due to a high rate of recurrence. Fibrotic Dupuytren's nodules originate within the affected hand's diseased aponeurosis, a robust network of fibrous tissue that interconnects the skin with the underlying structures of the hand, including bones and tendon sheaths. Typically devoid of pain, these nodules tend to align along the longitudinal axes, progressively forming strands that lead to finger contractures. This process ultimately culminates in significant constraints on hand function and a marked diminishment of the patient's quality of life [5]. Both conditions share similarities on a microscopic level, as well. For one, keloids and Dupuytren's disease show an increase of fibroblasts

* Corresponding author. Clinic of Hand Surgery, Helios Klinikum Muenchen West, Steinerweg 5, 81241, Munich, Germany.
E-mail address: elias_volkmer@hotmail.com (E. Volkmer).
[1] These authors are co-first authors.

https://doi.org/10.1016/j.heliyon.2023.e23681
Received 30 April 2023; Received in revised form 27 November 2023; Accepted 9 December 2023
Available online 13 December 2023

with an excessive extracellular matrix deposition, particularly collagen type I and III [5,6]. It is known that molecular changes in contractile myofibroblasts and regulation of matrix proliferation play a pivotal role in the evolution of both conditions, yet the cause of the diseases is not fully understood [3,4]. New therapeutic strategies, such as pharmacological injections, radiotherapy and ultrasound were tested, but their outcomes are unsatisfactory and inferior to surgical removal of the fibrotic tissue [2,7]. Based on these pathophysiological similarities, we hypothesized that common molecular characteristics may exist between Dupuytren's disease and keloid scars. In an attempt to detect similarities on a molecular level and to identify potential molecular targets for a non-surgical, potentially definitive therapy, in this study we applied high throughput next generation RNA-sequencing to three tissue samples of either condition.

2. Materials and methods

2.1. Ethics statement, sample acquisition and processing

This study was approved by the ethical commission of the Ludwig-Maximilians-University Munich (Project number 19–177). All six donors were at least 18 years old and signed informed consent prior to enrolment in the study. Human keloid scar tissue was obtained from three patients during either implant removal or surgical scar correction for aesthetical reasons. Keloids were classified as such by the surgeon and the study nurse independently. Three samples of Dupuytren's tissue were obtained during surgical correction of finger contractures. In Supplementary Table S1 detailed patient and sample information is listed. To ensure an appropriate RNA quality of the samples, all samples were processed immediately after dissection from the patient inside the operating room. The dissected samples were minced in a drop of ice cold and sterile 0.9 % sodium chloride solution in a Petri dish with a scalpel. Afterwards, tissue pieces were transferred to 5 ml TRIzol (Thermo Fisher, USA) in a 15 ml falcon tube and transferred to the laboratory for further processing. To loosen the cell structures, the tissue pieces were homogenized three times at 5000 rpm for 20 s using a high throughput tissue homogenizer (Precellys 24, Bertin Technologies, France). Afterwards, the homogenate was centrifuged at 12,000 g for 10 min at 4 °C to remove leftover extracellular matrix pieces. Finally, the supernatant was stored in a −80 °C freezer until sequencing library preparation.

2.2. RNA library preparation, sequencing and Bioinformatic analysis

For the total RNA isolation 5 ml TRIzol-tissue-homogenates (Directzol™) and the RNA MiniPrep Kit (Zymo Research, USA) with 96 % ethanol were used according to the manufacturer's protocol. Subsequently, the RNA integrity was validated with a BioAnalyzer (Agilent, USA). Following the instructions provided by the manufacturer, RNA-sequencing libraries were generated with the SENSE mRNA-Seq Library Prep Kit V2 (Lexogen, Austria). All libraries were sequenced on the same run with a HiSeq1500 device (Illumina, USA) at a read length of 50 bp and a sequencing depth of approximately 20 million reads per sample. The next step was to demultiplex the samples with the corresponding Illumina sequencing primers. After demultiplexing, reads were aligned against the human reference genome (release GRCh38.101) using STAR (version 2.7.2b) to establish read per gene counts for 60672 genes. Before processing the differentially expressed genes, the genes that were lower than 10 reads in the total of the whole samples were filtered out by the rowSum method [8] and the analysis was performed with the remaining 22914 genes. The gene expression was normalized using the variance stabilizing transformation (vst) method and the dimensionality was reduced with a principal component analysis (PCA) [9–11]. For differential gene expression analysis, the DESeq2 package (version 1.28.1) was used with a predefined p-adjusted value cut off of $\leq$0.05 and a Log2FoldChange cut off of $\pm$2 [12]. To generate the MA plots, we employed ggpubr [13]. The Venn diagram was constructed based on genes displaying significant differential expression, characterized by a p-adjusted value < 0.05. To identify significant Gene Ontology (GO) Biological Pathways, we conducted a Gene Set Enrichment Analysis (GSEA) for each condition. This was accomplished using the R package clusterProfiler (version 3.14) [14].

2.3. Functional enrichment analysis of DEGs

The list of significant DEGs was used to perform The Kyoto Encyclopedia of Genes and Genomes (KEGG) pathway analysis using the Database for Annotation Visualization and Integrated Discovery (DAVID) online tool [15,16]. Cut-off values were a p-value $<$0.05 and a gene count per annotated pathway $\geq$2.

2.4. Protein-protein-interaction (PPI) network and module analysis

The PPI network was constructed by using the Search Tool for the Retrieval of Interacting Genes (STRING) database based on all significantly up- or downregulated DEGs. A preset combined protein interaction score of $>$0.4 was selected on the STRING database as a cut-off value to construct the network. Cytoscape was used to visualize the network [17]. The biological significance of the modules was assessed using the Molecular Complex Detection (MCODE) plugin. The modules were ranked by their degree and selected with an MCODE score $>$5 and a number of nodes $>$6 [18]. A KEGG pathway enrichment analysis was conducted for the top 5 modules of the PPI network.

3. Results

3.1. Identification of DEGs and principal component analysis: keloids and Dupuytren's disease display entirely distinct expression profiles

We extracted high quality RNA from all tissue samples and identified a total of 1922 differentially expressed genes, which were statistically significant (padj. <0.05). Out of these 1922 genes, 1401 genes have been upregulated within the keloid scar samples whereas 521 genes have been upregulated within the Dupuytren's disease samples. A full list of all significantly DEGs can be found in the supplementary tables (Table S2). The principal component analysis (Fig. 1A) revealed a tight clustering among the Dupuytren samples, while greater variability was observed in the keloid group. Interestingly, despite clear clinical and microscopic similarities, we found absolutely no overlap between the two diseases. They displayed entirely distinct expression profiles. Fig. 1B depicts the Top 100 differentially expressed genes between both entities. Most of the genes belong to the family encoding for skin related processes, e.g., FLG2, which is essential for normal cell-cell adhesion and proper cornification [19]. IVL encodes the expression of the eponymous protein and contributes to the formation and protection of corneocytes [20]. In addition, it has a crucial role in normal skin, aberrant expression patterns of IVL have been found in keloid scar tissues and have been associated with increased epidermal thickness [21].

The Venn diagram in Fig. 2A shows that 1401 genes were significantly upregulated in keloid tissue and 521 genes were significantly upregulated in the Dupuytren's disease group. The diagram further shows that there was no overlap in significantly expressed genes. In total there were 13571 expressed genes. The MA plot (Fig. 2B) displays significantly and non-significantly expressed genes. In tissue samples of Dupuytren's disease several genes were significantly upregulated in comparison to keloid samples, e.g., HCN1 (Hyperpolarization Activated Cyclic Nucleotide Gated Potassium Channel 1; FC = 8.5, padj. < 0.05). Similarly, TREM1 (Triggering Receptor Expressed on Myeloid Cells 1; FC = 8.4, padj. < 0.05) and MYO3A (Myosin IIIA) transcripts (FC = 8.4, padj. < 0.05) were significantly upregulated. As expected, several transcripts of proteins relevant to skin related processes were significantly upregulated in keloid tissue as opposed to the Dupuytren's disease samples, namely, FLG2 (Filaggrin 2) (FC = 12.7, padj. < 0.05) and LCE2B (Late Cornified Envelope 2B) (FC = 11.4, padj. < 0.05).

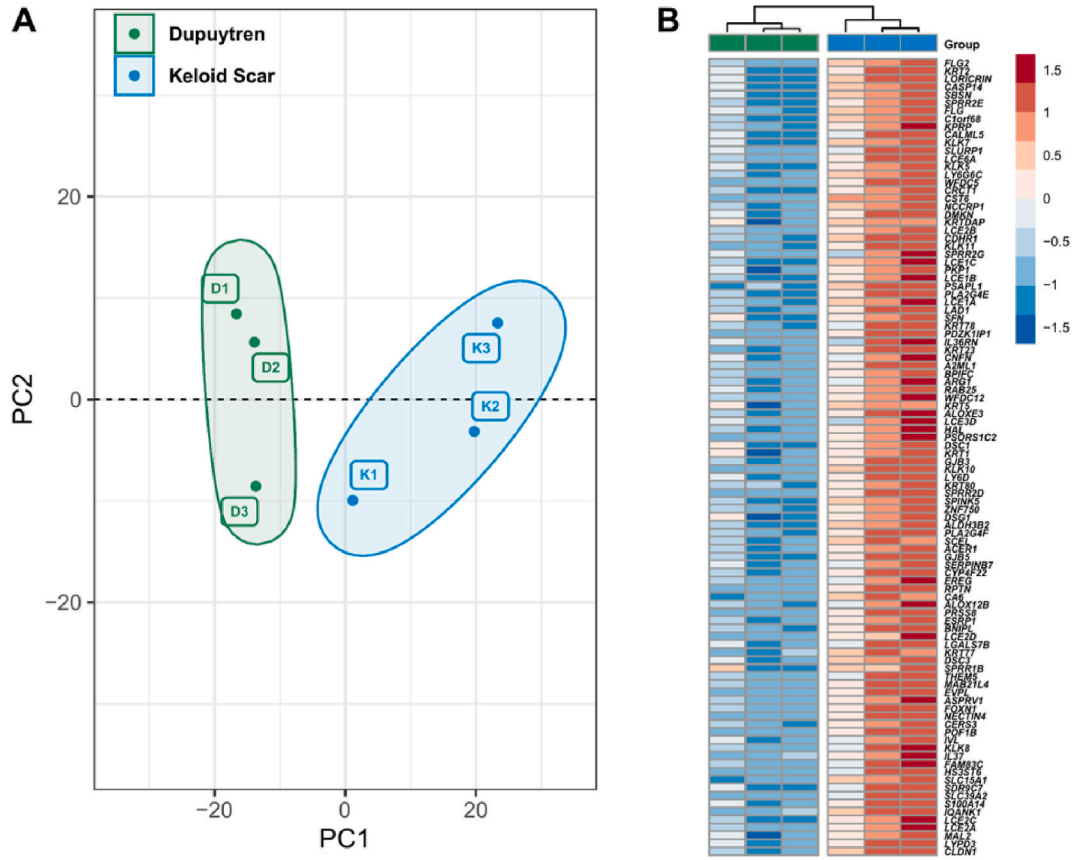

Fig. 1. A) A principal component analysis was performed on the regularized log transformed count data using DESeq2. Green dots represent the Dupuytren samples and blue dots the keloid samples. Despite clinical and microscopical similarities, there is absolutely no overlap between the two conditions. **B)** This figure represents a heatmap of differentially expressed genes between the keloid and Dupuytren samples. The Top 100 genes displayed in the map were clustered using the hierarchical average linkage clustering and Euclidean distances in the R package for Nonnegative Matrix Factorization.

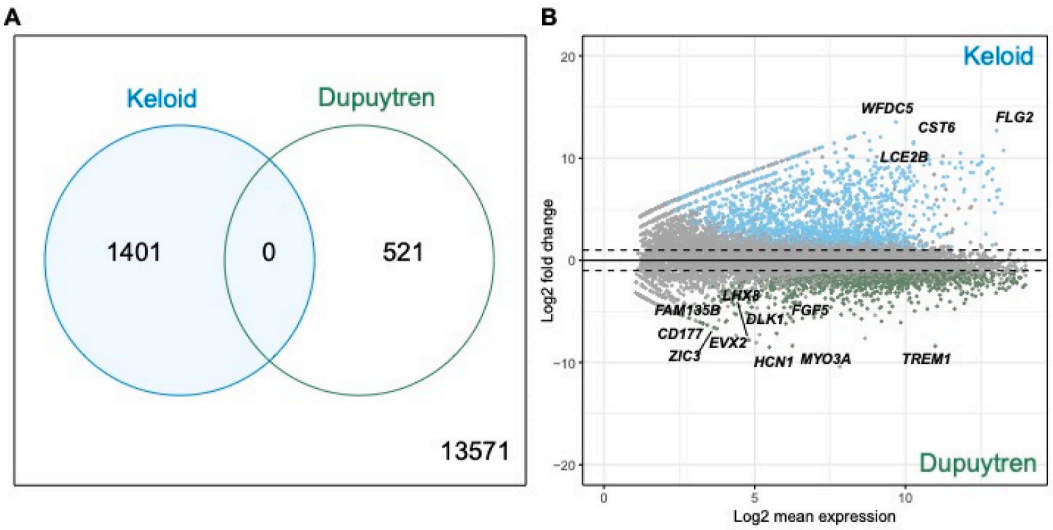

Fig. 2. A) The Venn-Diagram displays all differentially expressed genes and shows no overlap between Dupuytren's disease and keloid scar tissue samples. In total 13571 genes were expressed. **B)** The MA plot illustrates the upregulated genes of keloid scar and Dupuytren's disease samples. The data points above the x-axis depict upregulated genes in keloid scars, whereas data points below the x-axis show upregulated genes in Dupuytren tissue samples. Blue dots indicate significantly upregulated genes in keloid scar tissue, while green dots denote significantly upregulated genes in Dupuytren's disease tissue. Grey data points represent not significantly regulated genes.

3.2. GO functional enrichement analysis

To better undrstand the biological differences of the two conditions, we performed a functional enrichment analysis to determine dysregulated Gene Ontology (GO) categories (Fig. 3) [22,23]. The analysis unveiled a pronounced focus on metabolic processes related to glucan and glycogen within the Dupuytren group. The associated terms encompassed glycogen metabolic process (GO:0005977), cellular glucan metabolic process (GO:0006073) and glucan metabolic process (GO:0044042). Moreover, numerous functional biological processes relevant to tendon development such as tendon formation (GO:0035992), tendon cell differentiation (GO:0035990) and tendon development (GO:0035989) exhibited a pronounced concentration among patients affected by Dupuytren's disease. Notably, in keloid samples, processes involved in skin development (GO:0043588) and especially the epidermis (GO:0008544), as well as the differentiation of keratinocytes (GO:0030216) and associated epidermal cell differentiation (GO:0009913) were enriched. For a comprehensive list of all enriched GO terms, refer to the supplementary file (Table S3).

3.3. KEGG pathway analysis, GO functional enrichement analysis of selected pathways and construction of the PPI network including module analysis

A KEGG pathway analysis revealed 29 and 21 significantly enriched pathways (Table S4A and B) for keloids and Dupuytren's disease, respectively, including arachidonic acid metabolism, metabolic pathways, transcriptional dysregulation in cancer and cell adhesion molecules. The Top 5 KEGG pathways are shown in Table 1. In light of the considerable number of enriched genes within the KEGG pathway (hsa01100), we conducted a GO enrichment analysis using the DAVID online tool, employing default parameters based on annotated genes. The objective was to pinpoint pertinent biological processes. Notably, the analysis yielded a robust enrichment of GO terms associated with sphingolipid and eicosanoid metabolic processes. For a comprehensive rundown of these GO terms, please refer to the attached document (Table S5). Significant genes identified via KEGG and GO enrichment analysis were exemplarily visualized in the arachidonic acid metabolism (hsa00590) and the sphingolipid metabolism (hsa00600) pathway using the KEGG pathways maps online tool (Fig. S1).

For further analysis the list of significant DEGs was mapped using the STRING database to construct a PPI network. The Top 10 genes with the highest degrees were identified using the software Cytoscape, assuming that these play a major role in the pathogenesis (Table 2). The MCODE plug-in identified six modules with a score of >5 and more than 6 nodes. Fig. 4 illustrates the PPI network for Module2. The remaining networks can be accessed in supplementary files (Figs. S2–4).

For example, KEGG enrichment analysis of each module showed that the genes in Module 3 (including ALOX15, CYP2C9, PLA2G2F, PLA2G3, PLB1 ITGA3, COL4A3 and ITGA8) were associated with arachidonic acid metabolism, linoleic acid metabolism and ECM-receptor interaction. Table 3 provides a compilation of the Top 3 KEGG pathways associated with each module, ranked by their respective p-values. For Module 1 there were no annotated pathways. A list of all annotated KEGG pathways, which were associated with each individual module can be found in the attachment (Tables S6A–F).

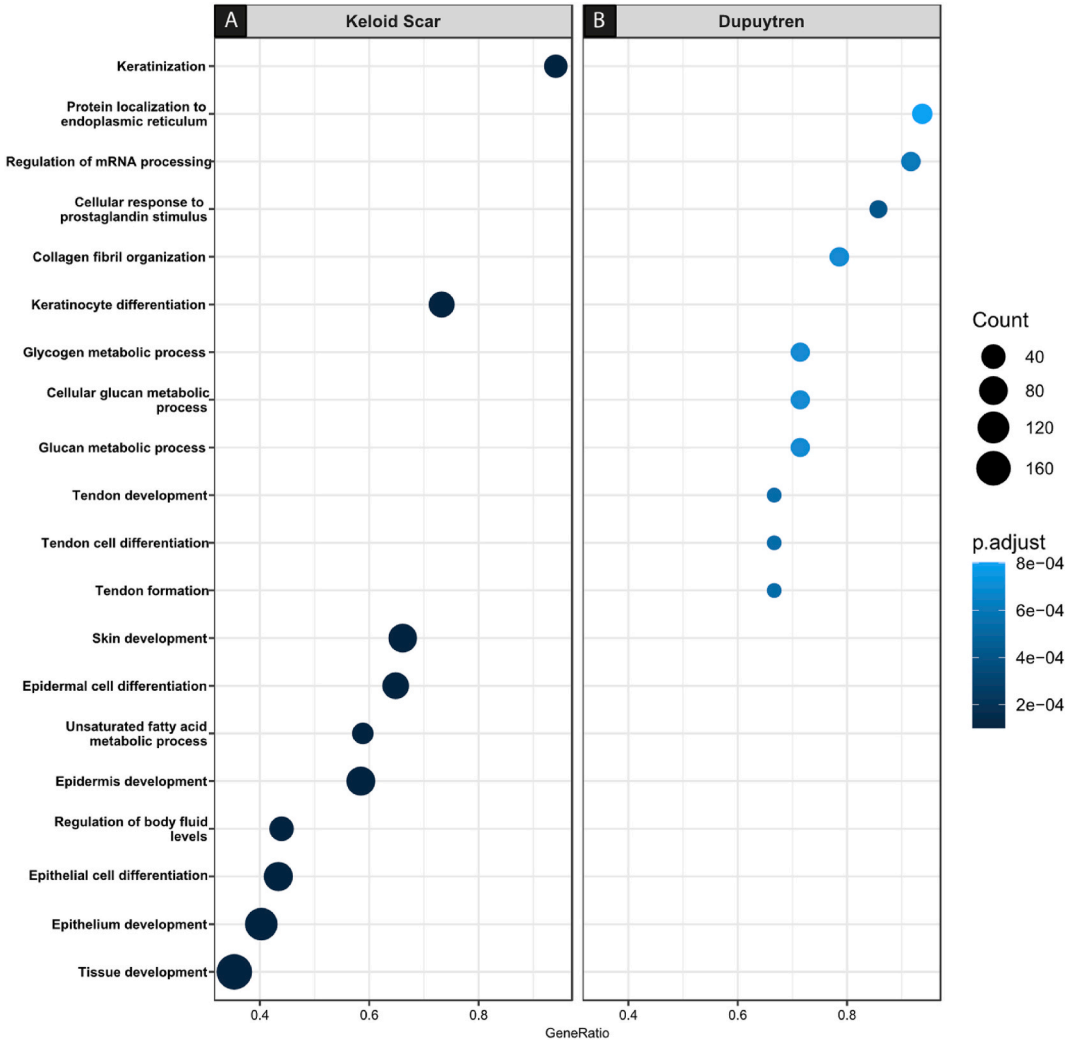

Fig. 3. Dot plot showing the Top 10 enriched GO biological processes of differentially expressed genes in keloid scars (A) and Dupuytren's disease (B). The processes are ranked according to the gene ratio. The Gene ratio is the proportion of genes that significantly correlated with the total number of genes associated to that process. The p-adjusted value is represented by the shading of the dots. The diameter of the dots represents the process specific gene count, which refers to the number of genes associated with each GO biological process.

Table 1
This table displays the KEGG pathway enrichment analysis of the DEGs of keloid scars and Dupuytren's disease samples using the Database for Annotation Visualization and Integrated Discovery (DAVID) online tool. The following cut-off criteria were applied: p-value <0.05 and a gene count ≥ 2.

KEGG pathway term	Description	No. of enriched genes	p-value
Upregulated in keloids			
hsa01100	Metabolic pathways	150	1.37×10^{-6}
hsa00590	Arachidonic acid metabolism	17	1.98×10^{-6}
hsa04530	Tight junction	25	4.51×10^{-4}
hsa00591	Linoleic acid metabolism	9	6.76×10^{-4}
hsa00600	Sphingolipid metabolism	12	7.32×10^{-4}
Upregulated in Dupuytren's samples			
hsa05171	Coronavirus disease - COVID-19	16	1.60×10^{-3}
hsa03010	Ribosome	13	1.85×10^{-3}
hsa05202	Transcriptional misregulation in cancer	14	2.25×10^{-3}
hsa04514	Cell adhesion molecules	12	3.61×10^{-3}
hsa04350	TGF-β signaling pathway	9	4.19×10^{-3}

Table 2
The Top 10 genes selected by the highest degree as calculated using Cytoscape.

Gene symbol	Gene name	Degree	Upregulated in
CDH1	Cadherin 1	332	Keloid
ERBB2	Erb-B2 Receptor Tyrosine Kinase 2	258	Keloid
EGF	Epidermal Growth Factor	256	Keloid
NOTCH1	Notch Receptor 1	200	Keloid
CASP3	Caspase 3	194	Dupuytren's disease
RPS27A	Ribosomal Protein S27a	192	Dupuytren's disease
CXCL8	C-X-C Motif Chemokine Ligand 8	180	Dupuytren's disease
IL10	Interleukin 10	180	Dupuytren's disease
SOX9	SRY-Box Transcription Factor 9	174	Keloid
ITGB1	Integrin Subunit Beta 1	174	Dupuytren's disease

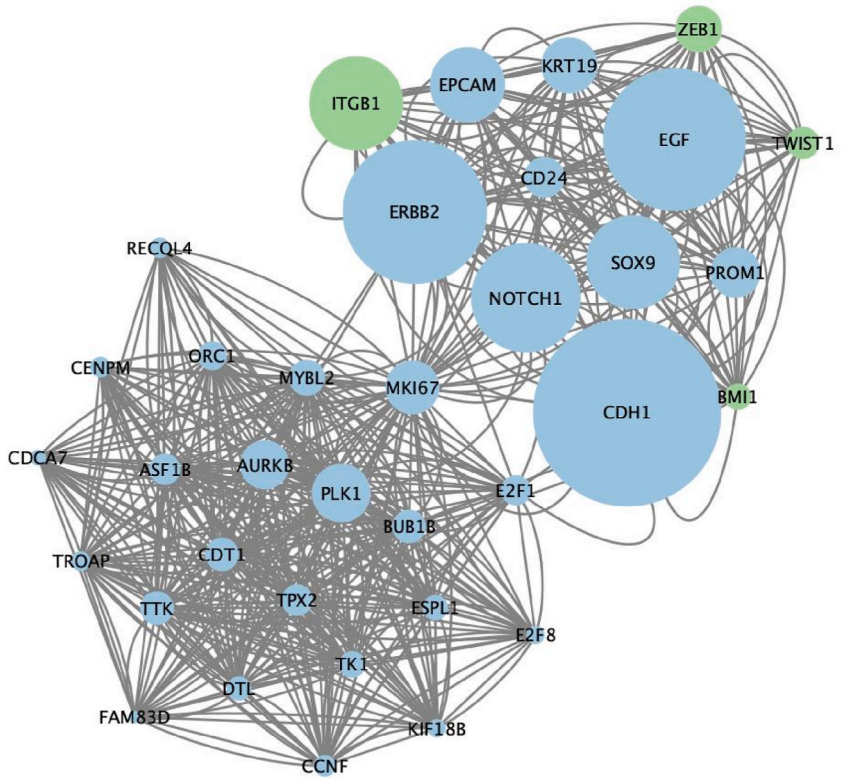

Fig. 4. Significant Modules identified with the MCODE plugin, Module 2 (MCODE score = 16.71, nodes = 35). Blue nodes represent significantly upregulated DEGs in keloids and green nodes represent DEGs within Dupuytren's samples respectively. The node diameter is proportional to the number of degrees of each node.

4. Discussion

Keloid scars and Dupuytren's disease share several clinical and microscopic similarities. For example, both conditions show an accumulation in different ethnic groups. Keloids occur in all races with a preponderance in Africans or people of African descent [24]. By contrast Dupuytren's disease is rare in Africans and mostly affects people of Caucasian descent [25]. Studies have shown that individuals with a positive family history are more susceptible to the disease, and they are more prone to developing an earlier onset coupled with a higher severity. These findings demonstrate a genetic predisposition in both conditions [3,26,27]. The diseases occur in different regions of the body. Whereas Dupuytren's disease mainly affects the aponeurosis of the palms of the hands and rarely the soles of the feet (which is then called Ledderhose's disease), keloids tend to occur within the skin of the chest, shoulders, chin, neck, lower legs and ears [4,5]. Although on a macroscopical level the affected regions appear to be quite distinct, microscopically both share common characteristics. Both keloid scars and Dupuytren's disease seem to form preferentially on mechanically stressed regions [5, 28]. Moreover the conditions are characterized by hyperproliferation of extracellular matrix, particularly collagen type I and III [29, 30]. On a molecular level, in both conditions transforming growth factor beta (TGF-β) has been extensively studied and seems to play a

Table 3
This table shows the top 3 KEGG pathways of significant modules identified using MCODE in Cystoscape and the DAVID online tool.

KEGG pathway term	Description	p-value	Genes
Module 2			
hsa04110	Cell cycle	8.02×10^{-6}	ESPL1, ORC1, PLK1, E2F1, BUB1B, TTK
hsa05219	Bladder cancer	1.06×10^{-4}	CDH1, EGF, ERBB2, E2F1
hsa05215	Prostate cancer	1.40×10^{-3}	ZEB1, EGF, ERBB2, E2F1
Module 3			
hsa00590	Arachidonic acid metabolism	4.73×10^{-21}	CYP2J2, PLA2G2F, PLA2G4F, PLA2G4D, PLA2G4E, PLA2G2A, CYP4F3, ALOX15, PLA2G3, ALOX12, ALOX12B, CYP4F8, ALOX15B, PLB1, PTGS1, CYP2C9
hsa00591	Linoleic acid metabolism	8.54×10^{-14}	CYP2J2, PLA2G2F, CYP2C9, PLA2G4F, PLA2G4D, PLA2G4E, ALOX15, PLA2G2A, PLA2G3, PLB1
hsa04512	ECM-receptor interaction	1.07×10^{-10}	COL2A1, ITGA3, ITGB4, COL4A3, ITGA8, COL4A6, COL4A5, COL9A3, ITGAV, ITGB7, ITGB6
Module 4			
hsa00600	Sphingolipid metabolism	3.60×10^{-11}	CERS3, SMPD3, SMPD2, CERS4, UGT8, ACER1, DEGS2, PLPP2, SGPP2
hsa04916	Melanogenesis	6.20×10^{-5}	DCT, TYRP1, WNT7A, MITF, TYR, WNT4
hsa04071	Sphingolipid signaling pathway	1.35×10^{-4}	CERS3, SMPD2, CERS4, ACER1, DEGS2, SGPP2
Module 5			
hsa05224	Breast cancer	2.13×10^{-6}	FGF5, NOTCH3, FGF16, WNT10A, WNT3A, WNT16, DLL1, FGF22, FGF10
hsa05200	Pathways in cancer	4.82×10^{-5}	NTRK1, NOTCH3, WNT10A, WNT3A, PTCH1, TGFA, WNT16, DLL1, FGF5, FGF16, FGFR3, FGF22, FGF10
hsa05226	Gastric cancer	2.38×10^{-4}	FGF5, FGF16, WNT10A, WNT3A, WNT16, FGF22, FGF10
Module 6			
hsa04151	PI3K-Akt signaling pathway	2.95×10^{-8}	GNG10, CHRM1, GNG2, ERBB3, LPAR5, PDGFD, PDGFC, LPAR1, LPAR2, LPAR3
hsa04072	Phospholipase D signaling pathway	1.69×10^{-5}	LPAR5, PDGFD, PDGFC, LPAR1, LPAR2, LPAR3
hsa04015	Rap1 signaling pathway	9.09×10^{-5}	LPAR5, PDGFD, PDGFC, LPAR1, LPAR2, LPAR3

major role in fibroblast proliferation [31,32]. Regardless of the ever-increasing scientific understanding, both diseases tend to have high recurrence rates, and no definitive cure for either condition has been found. In both cases, surgery remains the mainstay of treatment if joint contractures or aesthetic disturbances occur.

To identify potential molecular targets for therapy and to substantiate the known similarities on a molecular level, we have compared gene expression profiles of the two common fibrotic spectrum disorders. Furthermore, we evaluated the PPI networks and associated pathways, which may play a role in the onset and progression of both diseases.

Our findings suggest characteristic molecular alterations within the two conditions. Interestingly, we found absolutely no overlapping gene expression profiles between them. Our analysis unveiled key biological processes and signaling pathways that could potentially hold pivotal roles in driving their onset and progression. Additionally, we identified ten genes for each disease which appear to be of central importance in disease development. These genes may provide useful starting points for the development of new therapeutic agents.

Differential gene expression analysis revealed 1922 DEGs, including 1401 upregulated genes within the keloid tissue samples and only 521 upregulated genes within the Dupuytren's disease samples. Most upregulated genes were found in keloids, and most of them are mainly associated with skin development and related processes. The reason for the significantly lager fraction of upregulated genes compared to downregulated genes might be due to the great number of genes encoding for skin development and keratinization.

Enrichment analysis of the identified DEGs within the keloid samples revealed several significantly enriched KEGG pathways, including arachidonic acid metabolism, metabolic pathways, tight junctions, and linoleic acid metabolism. In line with our findings is that keloids bear higher levels of arachidonic acid when compared to skin of keloid-prone and non-keloid-prone patients [33]. Arachidonic acid has several downstream products including eicosanoids such as leukotrienes, prostanoids of prostaglandins, prostacyclins and thromboxanes. These molecules are believed to be proinflammatory in nature and thereby contributing to the formation of keloid scars [34]. Furthermore, we found an upregulation of lipid and sphingolipid metabolic processes further suggesting that both processes hold a significant role in chronic inflammation, potentially contributing to keloid formation [34,35]. Little is known about lipid metabolism and inflammation in keloids. Among the enriched KEGG pathways within the Dupuytren's cohort were cell adhesion molecules, transcriptional dysregulation in cancer and the TGF-β signaling pathway. The TGF-β signaling pathway plays an important role in keloid and Dupuytren's disease formation [36,37]. TGF-β is a pivotal component in producing the myofibroblast phenotype

which is responsible for aberrant collagen deposition and contraction in Dupuytren's disease and supposedly keloid scars [38–40]. Therefore, monitoring these signaling pathways may aid in the prediction of the progression of these two diseases.

A PPI network analysis of the DEGs revealed that CDH1, ERBB2, EGF, NOTCH1, CASP3, RPS27A, CXL8, IL10, SOX9 and ITGB1 hold key positions in the pathogenesis of Dupuytren's disease and keloid formation. CDH1, which encodes for the protein E-cadherin, had similar expression levels in keloid keratinocytes when compared to normal keratinocytes. The protein levels of E-cadherin are diminished in keloids and are lost in cancer cells undergoing endothelial-mesenchymal transition (EMT), indicating a switch to mesenchymal markers such as N-cadherin [41–43]. The oncogene ERBB2 was identified to be attenuated in keloids and is believed to play a major role in margin migration via neuregulin-1 (NRG1) [44]. EGF increases fibroblast proliferation and motility [45]. To the more, EGF alters TGF-β1 signaling, which is a major pathway in the pathogenesis of keloid formation, leading to accumulation of ECM components [46]. Although our studies indicate an upregulation of EGF signaling, the evidence in the literature is contradictory, with several studies also suggesting a decreased expression of EGF [47]. The highly conserved Notch pathway is essential to the regulation of key cellular processes and functions such as fibroblast cell proliferation and migration. Notch-1, a member of a family comprising four transmembrane receptors (Notch-1 to Notch-4), has been identified to be increasingly expressed in keloids and hypertrophic scar tissue when compared to normal skin [48–50]. Blocking of Notch signaling resulted in decreased scar formation and prevention of tissue fibrosis in an experimental setting [51,52]. Our results are in line with these findings and suggest a crucial role for Notch signaling in the development of keloids. In addition, SOX9, which is important for chondrogenesis, was significantly upregulated [53].

In a previous investigation, Jung et al. identified that terms related to collagen and ECM were enriched in tissue samples of patients suffering from Dupuytren's disease [54]. In the present study DEGs, including ITGB1, COL2A1, ITGA8 and ITGAV, were predominantly enriched in the ECM-receptor interaction pathway. In accordance with that, Layton et al. found that pericytes derived from Dupuytren's disease nodules express several integrin receptors including ITGB1 and ITGAV [55]. It may therefore be speculated that these pathways and genes contribute to the progression of Dupuytren's disease. In addition, a KEGG pathway analysis of each individual module revealed that pathways, which also play a role in the development of different cancerous diseases, appear to be enriched in the fibrotic diseases assessed in our study. Using PCR analysis, Docheva et al. showed that fibronectin-binding integrins β3 and β5 are upregulated in Dupuytren's disease [56].

It has to be kept in mind, however, that the sample size in our study was small and additional experiments, for example reverse transcription-quantitative polymerase chain reaction, were not performed to confirm mRNA expression levels. Thus, further studies are required to verify these genetic signatures.

5. Conclusion

Our study showed that Dupuytren's disease and keloids, despite some obvious similarities, share indubitably no overlapping gene expression profiles. Our results indicate that CDH1, ERBB2, EGF, NOTCH1 and SOX9 play a crucial role in the onset and development of keloids. On the other hand, CASP3, RPS27A, CXCL8, IL-10 and ITGB1 play a pivotal role in the pathogenesis of Dupuytren's disease.

We identified important upregulated KEGG pathways of both keloids and Dupuytren's disease, some of which haven't been described in the literature before and therefore warrant further investigation. They include metabolic pathways (hsa01100), arachidonic acid metabolism (hsa00590) and transcriptional dysregulation in cancer (hsa05202).

Funding

This research did not receive any specific grant from funding agencies in the public, commercial, or not-for-profit sectors.

Data availability statement

Data associated with our study has not been deposited into a publicly available repository. Data included in the article/supp. Material/referenced in the article will be made available upon request.

Declarations of Interest: none.

Ethics declarations

- This study was conducted in accordance with the Declaration of Helsinki and approved by the Ethics Committee of the LMU Medical Faculty (AZ 19–177).
- All participants/patients (or their proxies/legal guardians) provided informed consent to participate in the study.
- All participants/patients (or their proxies/legal guardians) provided informed consent for the publication of their anonymised case details and images.

CRediT authorship contribution statement

Marcus Stocks: Conceptualization, Data curation, Formal analysis, Investigation, Methodology, Visualization, Writing – original draft, Software. **Annika S. Walter:** Conceptualization, Data curation, Formal analysis, Investigation, Methodology, Software, Visualization, Writing – original draft. **Elif Akova:** Software, Visualization, Formal analysis. **Gerd Gauglitz:** Writing – review & editing. **Attila Aszodi:** Project administration, Resources, Supervision, Writing – review & editing. **Wolfgang Boecker:** Resources.

Maximilian M. Saller: Conceptualization, Funding acquisition, Methodology, Project administration, Resources, Supervision, Validation, Visualization, Writing – review & editing. **Elias Volkmer:** Conceptualization, Funding acquisition, Methodology, Project administration, Resources, Supervision, Validation, Writing – review & editing.

Declaration of competing interest

The authors declare that they have no known competing financial interests or personal relationships that could have appeared to influence the work reported in this paper.

Appendix A

The appendix is an optional section that can contain details and data supplemental to the main text—for example, explanations of experimental details that would disrupt the flow of the main text but nonetheless remain crucial to understanding and reproducing the research shown; figures of replicates for experiments of which representative data is shown in the main text can be added here if brief, or as Supplementary data. Mathematical proofs of results not central to the paper can be added as an appendix.

Appendix B

Figure S1 to Figure S4
Table S1.
Table S2.
Table S3.
Table S4 A and B.
Table S5.
Table S6A to Table S6F

Appendix C. Supplementary data

Supplementary data to this article can be found online at https://doi.org/10.1016/j.heliyon.2023.e23681.

References

[1] A.P. Kelly, Keloids, Dermatol Clin. 6 (1988) 413–424.
[2] G.C. Limandjaja, F.B. Niessen, R.J. Scheper, S. Gibbs, Hypertrophic scars and keloids: overview of the evidence and practical guide for differentiating between these abnormal scars, Exp. Dermatol. 30 (2021) 146–161, https://doi.org/10.1111/exd.14121.
[3] T.B. Layton, L. Williams, J. Nanchahal, Dupuytren's disease: a localised and accessible human fibrotic disorder, Trends Mol. Med. (22) (2022) S1471–S4914, https://doi.org/10.1016/j.molmed.2022.12.001, 00313–6.
[4] U. Betarbet, T.W. Blalock, Keloids: a review of etiology, prevention, and treatment, J Clin Aesthet Dermatol 13 (2020) 33–43.
[5] B. Shih, A. Bayat, Scientific understanding and clinical management of Dupuytren disease, Nat. Rev. Rheumatol. 6 (2010) 715–726, https://doi.org/10.1038/nrrheum.2010.180.
[6] S. Tan, N. Khumalo, A. Bayat, Understanding keloid pathobiology from a quasi-neoplastic perspective: less of a scar and more of a chronic inflammatory disease with cancer-like tendencies, Front. Immunol. 10 (2019) 1810, https://doi.org/10.3389/fimmu.2019.01810.
[7] J.R. Mella, L. Guo, V. Hung, Dupuytren's contracture: an evidence based review, Ann. Plast. Surg. 81 (2018) S97, https://doi.org/10.1097/SAP.0000000000001607. –S101.
[8] A. Dobin, C.A. Davis, F. Schlesinger, J. Drenkow, C. Zaleski, S. Jha, P. Batut, M. Chaisson, T.R. Gingeras, STAR: ultrafast universal RNA-seq aligner, Bioinformatics 29 (2013) 15–21, https://doi.org/10.1093/bioinformatics/bts635.
[9] R.A. Becker, J.M. Chambers, A.R. Wilks, The New S Language: a Programming Environment for Data Analysis and Graphics, Wadsworth & Brooks/Cole Advanced Books & Software, Pacific Grove, Calif, 1988.
[10] W.N. Venables, B.D. Ripley, W.N. Venables, Modern Applied Statistics with S, fourth ed., Springer, New York, 2002.
[11] K.V. Mardia, J.T. Kent, J.M. Bibby, Multivariate Analysis, Academic Press, London ; New York, 1979.
[12] M.I. Love, W. Huber, S. Anders, Moderated estimation of fold change and dispersion for RNA-seq data with DESeq2, Genome Biol. 15 (2014) 550, https://doi.org/10.1186/s13059-014-0550-8.
[13] A. Kassambara, Ggpubr: "Ggplot2" Based Publication Ready Plots. R Package Version 0.6.0, 2023. https://cran.r-project.org/web/packages/ggpubr/index.html.
[14] G. Yu, L.-G. Wang, Y. Han, Q.-Y. He, clusterProfiler: an R Package for comparing biological themes among gene clusters, OMICS A J. Integr. Biol. 16 (2012) 284–287, https://doi.org/10.1089/omi.2011.0118.
[15] D.W. Huang, B.T. Sherman, Q. Tan, J.R. Collins, W.G. Alvord, J. Roayaei, R. Stephens, M.W. Baseler, H.C. Lane, R.A. Lempicki, The DAVID Gene Functional Classification Tool: a novel biological module-centric algorithm to functionally analyze large gene lists, Genome Biol. 8 (2007) R183, https://doi.org/10.1186/gb-2007-8-9-r183.
[16] M. Kanehisa, S. Goto, KEGG: kyoto encyclopedia of genes and genomes, Nucleic Acids Res. 28 (2000) 27–30, https://doi.org/10.1093/nar/28.1.27.
[17] D. Szklarczyk, A.L. Gable, D. Lyon, A. Junge, S. Wyder, J. Huerta-Cepas, M. Simonovic, N.T. Doncheva, J.H. Morris, P. Bork, L.J. Jensen, C. von Mering, STRING v11: protein–protein association networks with increased coverage, supporting functional discovery in genome-wide experimental datasets, Nucleic Acids Res. 47 (2019) D607, https://doi.org/10.1093/nar/gky1131. –D613.
[18] G.D. Bader, C.W.V. Hogue, An automated method for finding molecular complexes in large protein interaction networks, BMC Bioinf. 4 (2003) 2, https://doi.org/10.1186/1471-2105-4-2.
[19] J. Mohamad, O. Sarig, L.M. Godsel, A. Peled, N. Malchin, R. Bochner, D. Vodo, T. Rabinowitz, M. Pavlovsky, S. Taiber, M. Fried, M. Eskin-Schwartz, S. Assi, N. Shomron, J. Uitto, J.L. Koetsier, R. Bergman, K.J. Green, E. Sprecher, Filaggrin 2 deficiency results in abnormal cell-cell adhesion in the cornified cell layers and causes peeling skin syndrome type A, J. Invest. Dermatol. 138 (2018) 1736–1743, https://doi.org/10.1016/j.jid.2018.04.032.

[20] R.L. Eckert, H. Green, Structure and evolution of the human involucrin gene, Cell 46 (1986) 583–589, https://doi.org/10.1016/0092-8674(86)90884-6.
[21] G.C. Limandjaja, L.J. Broek, T. Waaijman, H.A. Veen, V. Everts, S. Monstrey, R.J. Scheper, F.B. Niessen, S. Gibbs, Increased epidermal thickness and abnormal epidermal differentiation in keloid scars, Br. J. Dermatol. 176 (2017) 116–126, https://doi.org/10.1111/bjd.14844.
[22] Gene Ontology Consortium, The Gene Ontology resource: enriching a GOld mine, Nucleic Acids Res. 49 (2021), https://doi.org/10.1093/nar/gkaa1113. D325–D334.
[23] M. Ashburner, C.A. Ball, J.A. Blake, D. Botstein, H. Butler, J.M. Cherry, A.P. Davis, K. Dolinski, S.S. Dwight, J.T. Eppig, M.A. Harris, D.P. Hill, L. Issel-Tarver, A. Kasarskis, S. Lewis, J.C. Matese, J.E. Richardson, M. Ringwald, G.M. Rubin, G. Sherlock, Gene ontology: tool for the unification of biology. The Gene Ontology Consortium, Nat. Genet. 25 (2000) 25–29, https://doi.org/10.1038/75556.
[24] G.G. Gauglitz, H.C. Korting, T. Pavicic, T. Ruzicka, M.G. Jeschke, Hypertrophic scarring and keloids: pathomechanisms and current and emerging treatment strategies, Mol Med 17 (2011) 113–125, https://doi.org/10.2119/molmed.2009.00153.
[25] L. Michou, J.-L. Lermusiaux, J.-P. Teyssedou, T. Bardin, J. Beaudreuil, E. Petit-Teixeira, Genetics of Dupuytren's disease, Joint Bone Spine 79 (2012) 7–12, https://doi.org/10.1016/j.jbspin.2011.05.027.
[26] M. Hirata, Y. Kamatani, A. Nagai, Y. Kiyohara, T. Ninomiya, A. Tamakoshi, Z. Yamagata, M. Kubo, K. Muto, T. Mushiroda, Y. Murakami, K. Yuji, Y. Furukawa, H. Zembutsu, T. Tanaka, Y. Ohnishi, Y. Nakamura, BioBank Japan Cooperative Hospital Group, K. Matsuda, Cross-sectional analysis of BioBank Japan clinical data: a large cohort of 200,000 patients with 47 common diseases, J. Epidemiol. 27 (2017), https://doi.org/10.1016/j.je.2016.12.003. S9–S21.
[27] W. Lu, X. Zheng, X. Yao, L. Zhang, Clinical and epidemiological analysis of keloids in Chinese patients, Arch. Dermatol. Res. 307 (2015) 109–114, https://doi.org/10.1007/s00403-014-1507-1.
[28] T. Dohi, J. Padmanabhan, S. Akaishi, P.A. Than, M. Terashima, N.N. Matsumoto, R. Ogawa, G.C. Gurtner, The interplay of mechanical stress, strain, and stiffness at the keloid periphery correlates with increased caveolin-1/ROCK signaling and scar progression, Plast. Reconstr. Surg. 144 (2019), https://doi.org/10.1097/PRS.0000000000005717, 58e–67e.
[29] M.M. van Beuge, E.-J.P.M. ten Dam, P.M.N. Werker, R.A. Bank, Matrix and cell phenotype differences in Dupuytren's disease, Fibrogenesis Tissue Repair 9 (2016) 9, https://doi.org/10.1186/s13069-016-0046-0.
[30] P.D.H.M. Verhaegen, P.P.M. van Zuijlen, N.M. Pennings, J. van Marle, F.B. Niessen, C.M.A.M. van der Horst, E. Middelkoop, Differences in collagen architecture between keloid, hypertrophic scar, normotrophic scar, and normal skin: an objective histopathological analysis, Wound Repair Regen. 17 (2009) 649–656, https://doi.org/10.1111/j.1524-475X.2009.00533.x.
[31] A.Y. Zhang, K.D. Fong, H. Pham, R.P. Nacamuli, M.T. Longaker, J. Chang, Gene expression analysis of dupuytren's disease: the role of TGF-beta2, J. Hand Surg.: European 33 (2008) 783–790.
[32] Z. Deng, M. Subilia, I.L. Chin, N. Hortin, A.W. Stevenson, F.M. Wood, C.M. Prêle, Y.S. Choi, M.W. Fear, Keloid fibroblasts have elevated and dysfunctional mechanotransduction signaling that is independent of TGF-β, J. Dermatol. Sci. 104 (2021) 11–20, https://doi.org/10.1016/j.jdermsci.2021.09.002.
[33] L. Louw, Keloids in rural black South Africans. Part 3: a lipid model for the prevention and treatment of keloid formations, Prostaglandins Leukot. Essent. Fatty Acids 63 (2000) 255–262, https://doi.org/10.1054/plef.2000.0209.
[34] C. Huang, R. Ogawa, Roles of lipid metabolism in keloid development, Lipids Health Dis. 12 (2013) 60, https://doi.org/10.1186/1476-511X-12-60.
[35] C. Zang, Y. Liu, H. Chen, The sphingolipids metabolism mechanism and associated MolecularBiomarker investigation in keloid, CCHTS 26 (2023) 2003–2012, https://doi.org/10.2174/1386207326666221031114305.
[36] H. Nagar, S. Kim, I. Lee, S. Kim, S.-J. Choi, S. Piao, B.H. Jeon, S.-H. Oh, C.-S. Kim, Downregulation of CR6-interacting factor 1 suppresses keloid fibroblast growth via the TGF-β/Smad signaling pathway, Sci. Rep. 11 (2021) 500, https://doi.org/10.1038/s41598-020-79785-y.
[37] M.A. Badalamente, S.P. Sampson, L.C. Hurst, A. Dowd, K. Miyasaka, The role of transforming growth factor beta in Dupuytren's disease, J. Hand Surg. 21 (1996) 210–215, https://doi.org/10.1016/S0363-5023(96)80102-X.
[38] J.M. Carthy, TGFβ signaling and the control of myofibroblast differentiation: implications for chronic inflammatory disorders, J. Cell. Physiol. 233 (2018) 98–106, https://doi.org/10.1002/jcp.25879.
[39] M. Wong, V. Mudera, Feedback inhibition of high TGF-beta1 concentrations on myofibroblast induction and contraction by Dupuytren's fibroblasts, J Hand Surg Br 31 (2006) 473–483, https://doi.org/10.1016/j.jhsb.2006.05.007.
[40] N. Jumper, R. Paus, A. Bayat, Functional histopathology of keloid disease, Histol. Histopathol. 30 (2015) 1033–1057, https://doi.org/10.14670/HH-11-624.
[41] M.J. Wheelock, Y. Shintani, M. Maeda, Y. Fukumoto, K.R. Johnson, Cadherin switching, J. Cell Sci. 121 (2008) 727–735, https://doi.org/10.1242/jcs.000455.
[42] M. Zeisberg, E.G. Neilson, Biomarkers for epithelial-mesenchymal transitions, J. Clin. Invest. 119 (2009) 1429–1437, https://doi.org/10.1172/JCI36183.
[43] J.M. Hahn, K.L. McFarland, K.A. Combs, D.M. Supp, Partial epithelial-mesenchymal transition in keloid scars: regulation of keloid keratinocyte gene expression by transforming growth factor-β1, Burns Trauma 4 (2016) 30, https://doi.org/10.1186/s41038-016-0055-7.
[44] N. Jumper, T. Hodgkinson, R. Paus, A. Bayat, A role for neuregulin-1 in promoting keloid fibroblast migration via ErbB2-mediated signaling, Acta Derm. Venereol. 97 (2017) 675–684, https://doi.org/10.2340/00015555-2587.
[45] Y. Hu, J. Fu, X. Liu, X. Xue, ERK1/2 signaling pathway activated by EGF promotes proliferation, transdifferentiation, and migration of cultured primary newborn rat lung fibroblasts, BioMed Res. Int. 2020 (2020), 7176169, https://doi.org/10.1155/2020/7176169.
[46] S. Barrientos, O. Stojadinovic, M.S. Golinko, H. Brem, M. Tomic-Canic, Growth factors and cytokines in wound healing, Wound Repair Regen. 16 (2008) 585–601, https://doi.org/10.1111/j.1524-475X.2008.00410.x.
[47] B. Shih, E. Garside, D.A. McGrouther, A. Bayat, Molecular dissection of abnormal wound healing processes resulting in keloid disease, Wound Repair Regen. 18 (2010) 139–153, https://doi.org/10.1111/j.1524-475X.2009.00553.x.
[48] F. Syed, A. Bayat, Notch signaling pathway in keloid disease: enhanced fibroblast activity in a Jagged-1 peptide-dependent manner in lesional vs. extralesional fibroblasts, Wound Repair Regen. 20 (2012) 688–706, https://doi.org/10.1111/j.1524-475X.2012.00823.x.
[49] W. Xia, B. Pan, B. Liu, X. Zhang, F. Ma, Y. Wang, X. Yang, D. Liu, S. Guo, [Expression of Notch receptors, ligands and downstream target genes in epidermis of hypertrophic scar], Zhonghua Zhengxing Waike Zazhi 25 (2009) 41–45.
[50] S. Lee, S.K. Kim, H. Park, Y.J. Lee, S.H. Park, K.J. Lee, D.G. Lee, H. Kang, J.E. Kim, Contribution of autophagy-notch1-mediated NLRP3 inflammasome activation to chronic inflammation and fibrosis in keloid fibroblasts, Int. J. Mol. Sci. 21 (2020) E8050, https://doi.org/10.3390/ijms21218050.
[51] C. Dees, P. Zerr, M. Tomcik, C. Beyer, A. Horn, A. Akhmetshina, K. Palumbo, N. Reich, J. Zwerina, M. Sticherling, M.P. Mattson, O. Distler, G. Schett, J.H. W. Distler, Inhibition of Notch signaling prevents experimental fibrosis and induces regression of established fibrosis, Arthritis Rheum. 63 (2011) 1396–1404, https://doi.org/10.1002/art.30254.
[52] J.-S. Diao, X. Zhang, J. Ren, H.-F. Zeng, B. Liu, F.-C. Ma, Y.-M. Wang, X.-T. Yang, S.-Z. Guo, W. Xia, [Blocking of Notch signaling decreased scar formation in rabbit ear hypertrophic scar model], Zhonghua Yixue Zazhi 89 (2009) 1088–1092.
[53] M. Naitoh, H. Kubota, M. Ikeda, T. Tanaka, H. Shirane, S. Suzuki, K. Nagata, Gene expression in human keloids is altered from dermal to chondrocytic and osteogenic lineage, Gene Cell. 10 (2005) 1081–1091, https://doi.org/10.1111/j.1365-2443.2005.00902.x.
[54] J. Jung, G.W. Kim, B. Lee, J.W.J. Joo, W. Jang, Integrative genomic and transcriptomic analysis of genetic markers in Dupuytren's disease, BMC Med. Genom. 12 (2019) 98, https://doi.org/10.1186/s12920-019-0518-3.
[55] T.B. Layton, L. Williams, N. Yang, M. Zhang, C. Lee, M. Feldmann, G. Trujillo, D. Furniss, J. Nanchahal, A vasculature niche orchestrates stromal cell phenotype through PDGF signaling: importance in human fibrotic disease, Proc. Natl. Acad. Sci. U.S.A. 119 (2022), e2120336119, https://doi.org/10.1073/pnas.2120336119.
[56] D. Docheva, B. Vaerst, S. Deiler, R. Giunta, M. Schieker, E. Volkmer, Veränderung des Zell-Phänotyps durch Morbus Dupuytren - eine in-vitro-Analyse, Handchir. Mikrochir. Plast. Chir. 44 (2012) 59–66, https://doi.org/10.1055/s-0032-1309025.